

Electronic Supplementary Information

**Quantification of ion transport mechanism in protective polymer coatings
on lithium metal anodes**

Hongyao Zhou,^{a†} Haodong Liu,^a Xing Xing,^a Zijun Wang,^b Sicen Yu,^a Gabriel M. Veith,^c and Ping Liu^{a*}

a. Department of NanoEngineering, 9500 Gilman Drive, La Jolla, California 92093, United States

b. Materials Science and Engineering Program, University of California San Diego

c. Material Science and Technology Division, Oak Ridge National Laboratory, Oak Ridge, Tennessee 37831, United States

† Present address: Department of Chemistry, Graduate School of Science, The University of Tokyo, Hongo, Bunkyo-ku, Tokyo 113-0033, Japan

Corresponding author: Ping Liu, piliu@ucsd.edu

Table of Contents

Table of Contents	2
Experimental methods	4
1. Materials	4
2. Preparation of cross-linked PAN–PBD film.....	4
3. Characterization and swelling test of the cross-linked PAN–PBD film.....	4
4. Electrochemical measurement of the cross-linked PAN–PBD film.....	5
5. Characterization of the Li deposits	5
6. Tensile and rheological measurements	5
Figure S1	6
Figure S2.....	7
Figure S3.....	8
Figure S4.....	9
Figure S5.....	10
Figure S6.....	11
Appendix A.....	12
Table A.....	12
Appendix B.....	13
Table B.....	13
Appendix C.....	14
Figure S7.....	14
Appendix D.....	15
Figure D1	15
Figure D2	15
Table D.....	16
Figure S8.....	17
Figure S9.....	18
Figure S10.....	19
Figure S11.....	20
Figure S12.....	21
Figure S13.....	22
Figure S14.....	23
Figure S15.....	24
Figure S16.....	25
Figure S17.....	26

Figure S18.....	27
Figure S19.....	28
Figure S20.....	29
Figure S21.....	30
Figure S22.....	31
Figure S23.....	32
References.....	33

Experimental methods

1. Materials

Poly(acrylonitrile-*co*-butadiene) (37–39wt% acrylonitrile content, Sigma Aldrich, U.S.), lithium sulfide (Li₂S, 99.98%, Sigma Aldrich,) elemental sulfur (S, sublimed, Fisher scientific), lithium bis(fluorosulfonyl)imide (LiFSI, battery grade, Capchem, China), lithium hexafluorophosphate (LiPF₆, battery grade, BASF, Germany), lithium perchlorate (LiClO₄ ≥ 95.0% Sigma Aldrich), dimethoxyethane (DME, battery grade, BASF), dimethyl carbonate (DMC, battery grade, BASF), ethylene carbonate (EC, battery grade, BASF), and fluoroethylene carbonate (FEC, battery grade, Capchem) were used as received. Tetrahydrofuran (THF, reagent grade, Spectrum Chemical, U.S.) and dimethyl formamide (DMF, reagent grade, Spectrum Chemical) were dried with activated molecular sieve (4A, Spectrum Chemical) prior to the use. Cu (9 μm) and Li (250 μm) foils were supplied from MTI Corporation, U.S., and Xiamen Tob New Energy Technology Co. LTD, China, respectively.

2. Preparation of cross-linked PAN–PBD film

The cross-linking reaction was performed inside the argon-filled glove box (H₂O < 0.5 ppm, O₂ < 1 ppm). 2.0 g of PAN–PBD was dissolved in 18 g of THF to obtain 10wt% PAN–PBD solution (stock solution **1**). 0.37 g (8.0 mmol) of Li₂S and 0.51 g (16 mmol) of S were dissolved in 4.0 mL of DMF to obtain Li₂S₃ (2 mol dm⁻³) solution (stock solution **2**). Varied volume of the solution **2** (0–1.7 mL) was added into the solution **1** (4.5 g) to obtain a mixed solution **3** with various Li₂S₃/AN (0–1.0 mol/mol). The weight ratio of THF/DMF in the mixed solution **3** was kept constant at 2.3 by dilution with additional DMF. Then, the mixed solution **3** was poured into a Teflon-coated petri dish and heated at 100 °C for 30 hours to complete the cross-linking reaction. THF and DMF were evaporated during the heating and a dark-colored, free-standing film was obtained. The typical thickness of the cross-linked PAN–PBD film ranged between 100 and 200 μm. After the cross-linking, the film was immersed in DME solvent for three days (which was replaced each day) to extract any residual DMF and unreacted polysulfides. A thinner film with typical thickness of approximately 10 μm was prepared by coating 60 μL of the mixed solution **3** on a stainless-steel substrate (2 cm²) and heated at 100 °C for 20 hours to complete the cross-linking reaction. The film was immersed in DMF to enable the peeling-off from the substrate and rinsed in DMC for several times (Figure S12, SI).

3. Characterization and swelling test of the cross-linked PAN–PBD film

The chemical bonding in the cross-linked PAN–PBD film was analyzed with attenuated total reflectance (ATR)-FTIR (UATR 2, PerkinElmer, U.S.). The swelling ratio of cross-linked PAN–PBD film was measured by comparing the area of the film before and after being immersed in the electrolyte solution. Cross-linked PAN–PBD film was cut into a circle shape (diameter = 13–16 mm) and immersed in the solvents (DME, DMC, DMC + EC) for 24 hours. The influence of the additional salts (LiFSI, LiPF₆, LiClO₄) was evaluated by transferring the film fully swollen in the solvents to the salt-added electrolyte solution. The swollen film was placed between two glass plates, and the optical image was recorded (Figure S21, SI). The area was directly evaluated from the digitized image, using an image processing software (ImageJ ver. 1.51h, N.I.H., U.S.). The swelling ratio is converted from the area ratio (A/A_0) to the volume ratio (V/V_0), under the assumption of the isotropic volume change: $V/V_0 = (A/A_0)^{3/2}$. The results obtained from 2–4 samples at each Li₂S₃/AN ratio were averaged, and the standard deviation was evaluated.

4. Electrochemical measurement of the cross-linked PAN–PBD film

Potentiostatic electrochemical impedance spectroscopy (PEIS) and chronoamperometry (CA) were carried out with the potentiostat (VSP-300 Biologic Instruments, U.S.). The Li deposition/dissolution cycles was carried out with the battery cycler (BT2000, Arbin Instruments, U.S.). The t_+ of PAN–PBD film was evaluated by a potentiostatic polarization method reported by Newman and Balsara.³⁴ The cross-linked PAN–PBD film was swollen in DME/LiFSI (1 mol kg⁻¹) or DMC/EC(1:1 in weight ratio)/LiPF₆ (1 mol kg⁻¹) and placed between two Li metal foils. Prior to the measurement, the Li was deposited/dissolved at 20 $\mu\text{A cm}^{-2}$ for 2 hours and 5 cycles to stabilize the Li/electrolyte interface. At the open-circuit voltage (OCV), 10 mV of the voltage polarization was applied at a frequency range from 1 MHz to 1 Hz to evaluate the bulk and interface resistances (R_{bulk} , R_{int}). A constant voltage of ± 5 and ± 10 mV for 2 hours was applied to obtain the steady-state current (I_{ss}). The t_+ was evaluated from the results obtained in the two measurement (see Appendix D for the detailed calculation in SI). The conductivity of was measured by the PEIS method described above with two stainless-steel blocking electrodes. The temperature of the cell was controlled by the ribbon heater and the Peltier cooler. The Li deposition was carried out in CR 2032-coin cell with a Cu foil (9 μm) as the working electrode and Li foil (250 μm) as the counter/reference electrode. The PAN–PBD thin film (10 μm) and a polypropylene battery separator (25 μm , Celgard, U.S.) was placed between the Cu and Li electrodes (see Figure S12 in SI). The electrolyte used for the Li deposition was DMC + EC (1:1 in weight ratio) + LiPF₆ (1 mol kg⁻¹) + FEC (5wt%). 60 μL of the electrolyte was added in the coin cell in all the experiment.

5. Characterization of the Li deposits

The morphology of the Li deposits and the PAN–PBD thin film were observed under the scanning electron microscope (SEM, Sigma 500, Zeiss Instruments, Germany) at the electron high tension (EHT) voltage of 3 kV, and through the in-lens detector. Surface chemistry on the Li deposits was probed using a PHI 3056 X-ray photoelectron spectrometer equipped with a dual Al K α (1486.7 eV) and Mg K α (1256.6 eV) anode source, operated at 350 W, and with sample chamber pressure below 10–8 Torr. Samples were disassembled in an argon-filled glovebox, rinsed with a small quantity of anhydrous DME (Sigma-Aldrich), and transferred to the XPS chamber using an airtight vacuum transfer system. High resolution scans were acquired using a pass energy of 23.5 eV and an energy step of 0.05 or 0.075 eV. Survey scans were measured using a pass energy of 93.5 eV and a 0.5 eV energy step. The binding energies were calibrated by setting the hydrocarbon C 1s (C–C, C–H) signal to 284.6 eV, which corresponds mainly to the adventitious carbon. C signal was measured before and after any other signal to precisely calibrate the energy scale.

6. Tensile and rheological measurements

Tensile strength of the cross-linked PAN–PBD at the dry state was evaluated with the tensile tester (Model 5982, Instron, U.S.), at a constant strain rate of 2 mm min⁻¹ (see Figure S22 in SI for the sample dimension). Rheological properties of the cross-linked PAN–PBD film were characterized using the Discovery HR-3 Rheometer (TA Instruments, U.S.) equipped with a 20 mm parallel-plate geometry. An oscillation frequency of 1 Hz was used in the amplitude sweep and an oscillation strain of 0.1% was used in the frequency sweep. During all the measurements, an axial force of 1 N was applied for proper contact between the sample and the plates. All the measurements are conducted at 25°C. Non-corrosive LiClO₄ was used as the electrolyte salt at the concentration of 1 mol kg⁻¹ in DMC/EC, and 0.3 mol kg⁻¹ in DME (saturated).

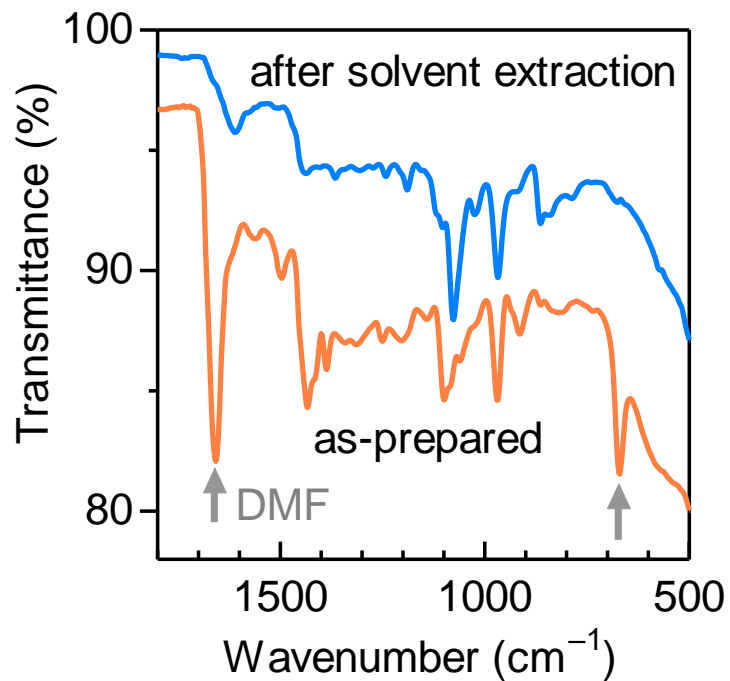


Figure S1. FTIR spectra of cross-linked PAN-PBD ($\text{Li}_2\text{S}_3/\text{AN} = 1.0$) before and after the solvent extraction in DME, showing a complete removal of DMF (the solvent used in the cross-linking step).

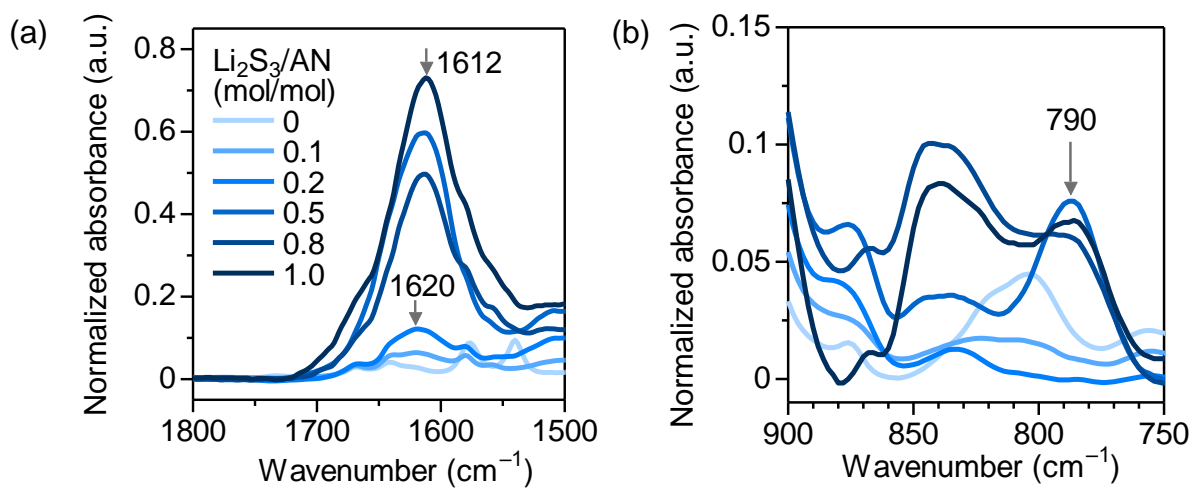


Figure S2. (a) Red shift of the C=C/C=N stretching peaks, indicating the extension of the conjugation length at higher Li₂S₃/AN ratio. (b) Appearance of the 1,2,3-trisubstituted =C-H bending at 790 cm⁻¹ at Li₂S₃ > 0.5.

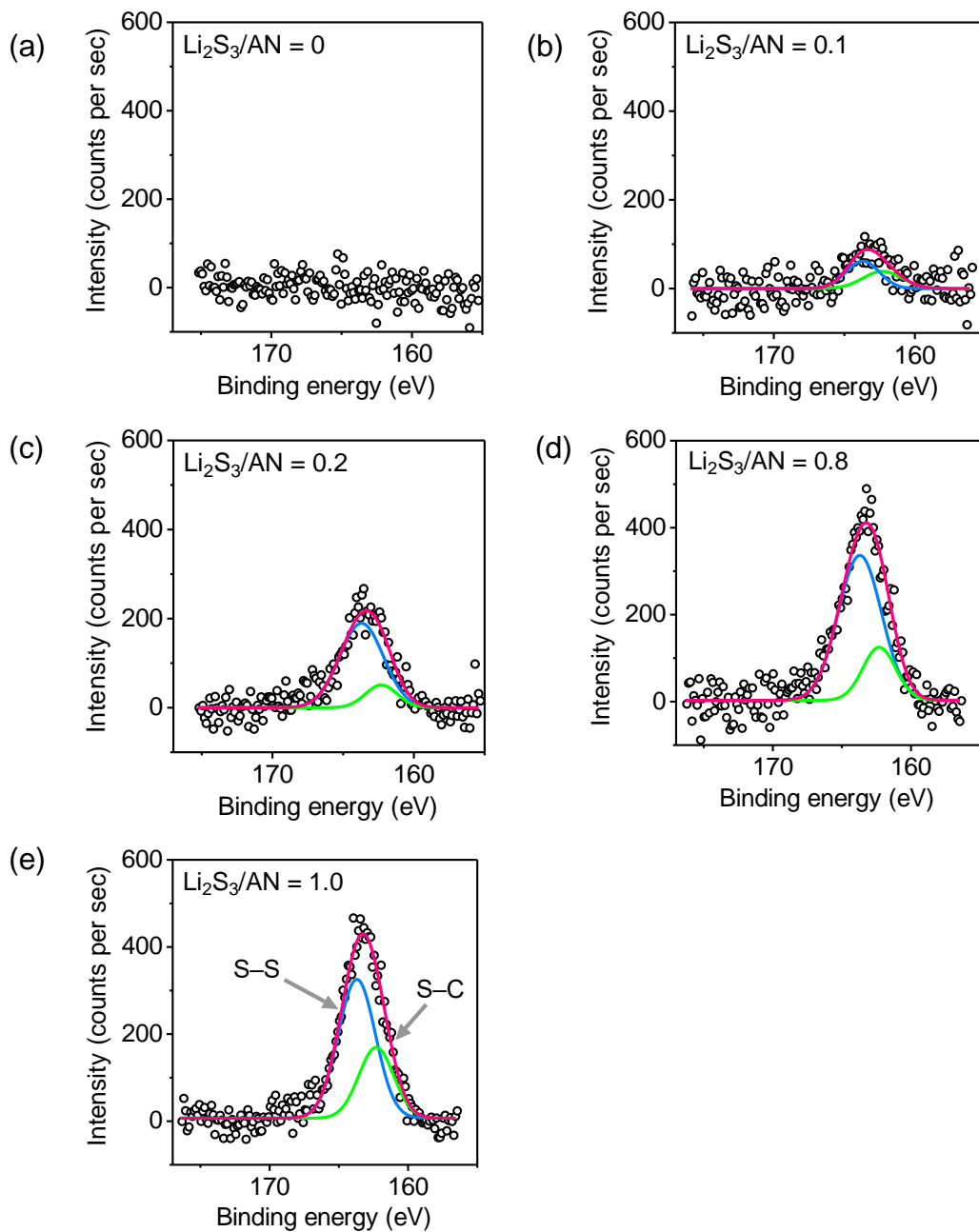
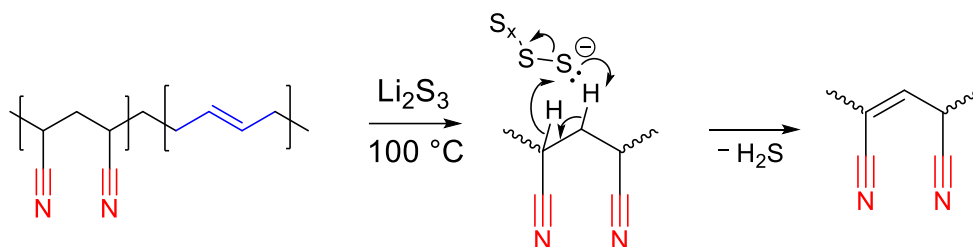
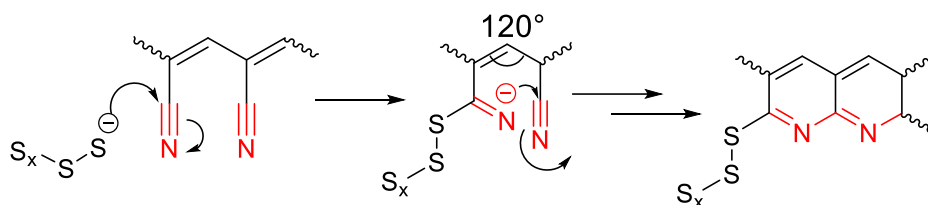


Figure S3. (a–e) XPS S 2p spectra of PAN–PBD after the solvent extraction in DME (polysulfide dissolves in DME). The deconvolution of the S 2p_{3/2} peak at 163.3 eV suggest the possible formation of both S–S (peak at 163.7 eV) and S–C (peak at 162.3 eV)¹ bonding with increasing $\text{Li}_2\text{S}_3/\text{AN}$ ratio (0–1.0).

1. Dehydrogenation of PAN main chain



2. Intramolecular cyclization



3. Intermolecular cross-linking

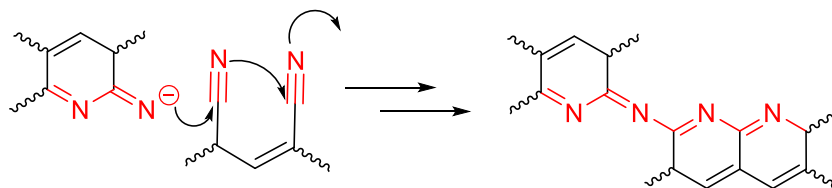


Figure S4. Reaction scheme of the cross-linking reaction of PAN–PBD catalyzed by Li_2S_3

1) Nucleophilic attack of polysulfide (S_x^-) on β -hydrogen of PAN results in dehydrogenation and production of H_2S gas.

2) Nucleophilic attack on $\text{C}\equiv\text{N}$ produces $\text{S}_x-\text{C}=\text{N}^-$ anion. The hydrogenation and formation of the $\text{C}=\text{C}$ in step (1) fixes the bonding angle of PAN main chain to 120° (angle of six-membered ring) and sterically facilitates intramolecular cyclization of $\text{C}\equiv\text{N}$.

3) The cyclization reaction initiated in step (2) transfers to different PAN chains and forms intermolecular cross-links.

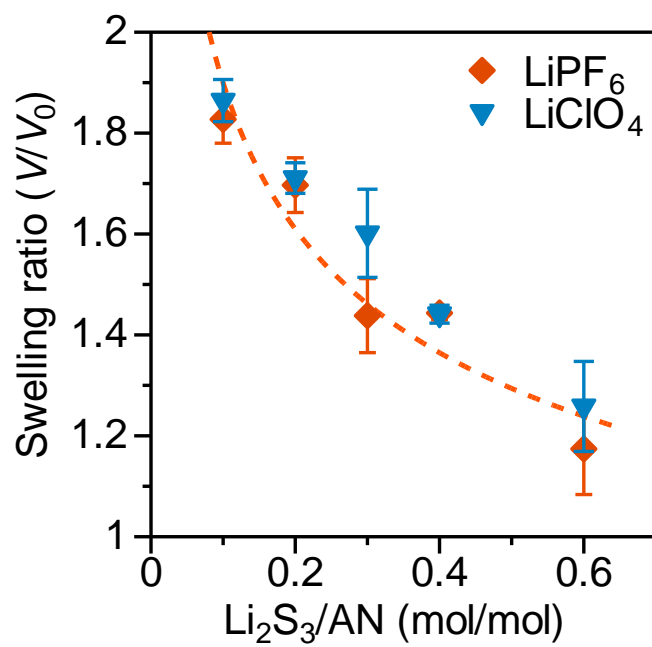


Figure S5. Swelling ratio of cross-linked PAN-PBD in DMC/EC mixed solvent added with LiClO₄ or LiPF₆ (1 mol kg⁻¹)

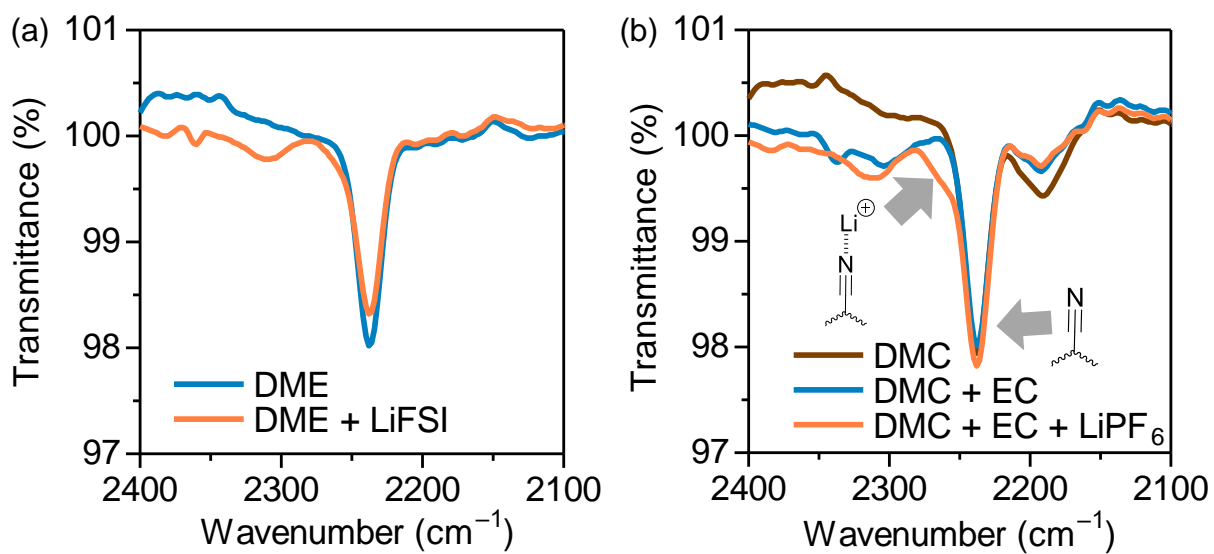


Figure S6. FTIR spectra of cross-linked PAN-PBD ($\text{Li}_2\text{S}_3/\text{AN} = 0.1$) swollen in (a) DME (+ LiFSI, 1 mol kg^{-1}), and (b) DMC, DMC + EC (+ LiPF_6 , 1 mol kg^{-1}).

Appendix A. Calculation of relative energy difference (RED) between polymer and solvent

HSPs are composed of three independent parameters, which account for dispersion force (δ_D), dipole-dipole interaction (δ_P), and hydrogen-bonding (δ_H), respectively (Table A). The sum of the squared values of HSPs equals to Hildebrand solubility parameter (δ).

$$\delta^2 = \delta_D^2 + \delta_P^2 + \delta_H^2 \quad (\text{A1})$$

RED is expressed as a ratio of R_a to R_o :

$$\text{RED} = \frac{R_a}{R_o} \quad (\text{A2})$$

where R_o is a constant related to the solubility of polymers. R_a is expressed as

$$R_a^2 = 4(\delta_{D1} - \delta_{D2})^2 + (\delta_{P1} - \delta_{P2})^2 + (\delta_{H1} - \delta_{H2})^2 \quad (\text{A3})$$

where the subscript 1 and 2 represents the HSPs of the solvent and the polymer, respectively.

The HSPs for the mixed solvent (e.g. solvent a + solvent b) can be calculated by taking the volume average of the HSPs of each solvent:

$$\delta_{i,a+b} = v_a \delta_{i,a} + v_b \delta_{i,b}$$

where $i = D, P, H$, and v_a and v_b is the volume ratio of the solvent. Note EC/DMC = 1/1 in weight ratio converts to 0.448/0.552 in volume ratio.

Table A. Values of HSPs, R_o , and V_1 used in this study²

	δ_D	δ_P	δ_H	R_o	V_1 (cm ³ mol ⁻¹)
PBD	17.5	2.3	3.4	6.5	-
PAN	21.7	14.1	9.1	10.9	-
DME	15.4	6.0	6.0	-	104.5
DMC	15.5	3.9	9.7	-	84.2
EC	19.4	21.7	5.1	-	66
DMC + EC (1:1 wt)	17.2	11.9	7.6	-	75 (averaged)

Appendix B. Calculation of χ parameter between polymer and solvent

Flory–Huggins χ parameter can be calculated from the HSPs:

$$\chi_{12} = \frac{\alpha V_1}{RT} [(\delta_{D1} - \delta_{D2})^2 + 0.25(\delta_{P1} - \delta_{P2})^2 + 0.25(\delta_{H1} - \delta_{H2})^2] \quad (\text{B1})$$

where α is an empirical parameter. Previously, $\alpha = 0.6$ was reported in the literature and therefore is used in this study.^{3,4}

Using Equation (A2) and (A3),

$$\chi_{12} = \frac{\alpha V_1}{RT} \left(\frac{R_a}{2}\right)^2 = \frac{\alpha V_1}{RT} \left(\frac{R_o \text{RED}}{2}\right)^2 \quad (\text{B2})$$

Equation (B2) shows the χ parameter is proportional to the RED squared. Calculated values of the χ_{12} parameters between each of the solvent and the polymer are listed in Table B. The χ_{12} of PAN–PBD copolymer is estimated from the volume average of χ_{12} of the two polymers (AN = 38wt% is used in this study and corresponds to 32vol%).

Table B. Calculated values of χ_{12} parameters between the solvents (DME, DMC, DMC/EC) and the polymers (PBD, PAB, PAN–PBD)

	PBD	PAN	PAN–PBD (AN = 38wt%)
DME	0.241	1.48	0.640
DMC	0.297	1.32	0.625
DMC + EC (1:1 wt)	0.498	0.392	0.464

Appendix C. Parameter fittings for σ_0 and ϕ_0 by using percolation model

In percolation model, the ionic conductivity is expressed as

$$\sigma = \sigma_0(\phi_{\text{LE}} - \phi_0)^n \quad (\text{Eq. 3})$$

Taking the power of $1/n$ for both sides of the equation gives

$$\sigma^{1/n} = \sigma_0^{1/n} \phi_{\text{LE}} - \sigma_0^{1/n} \phi_0 \quad (\text{C1})$$

In the linear fitting of $\sigma^{1/n}$ with respect to ϕ_{LE} , σ_0 , and ϕ_0 can be evaluated from the slope, and the x -intercept, respectively. The best fit is obtained with $n = 2$ for both ether and carbonate electrolytes (Figure S7)

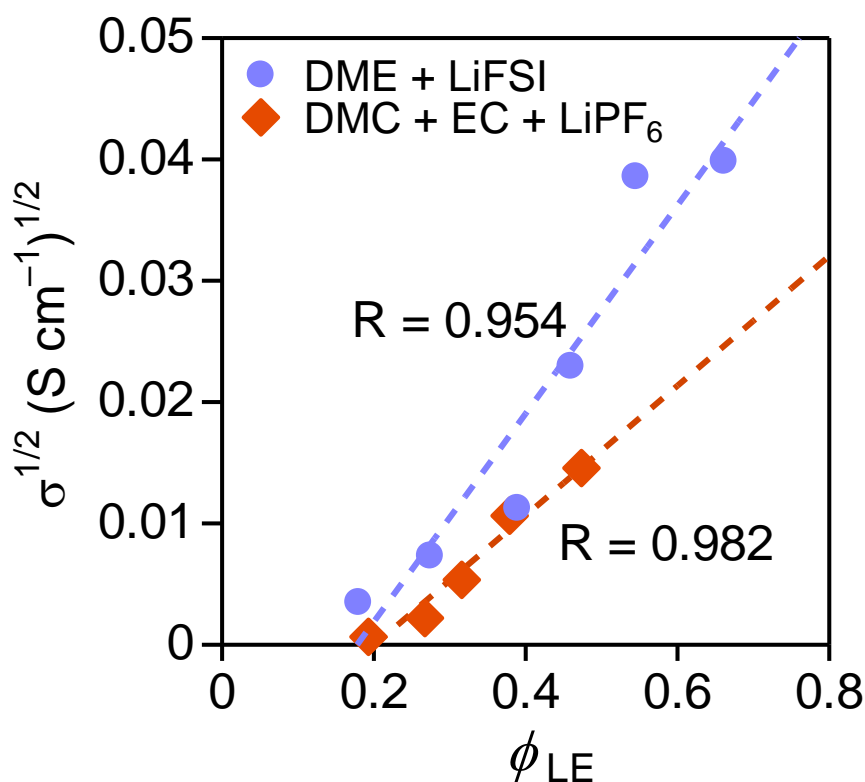


Figure S7. Fitting of $\sigma^{1/2}$ with respect to $\phi_{\text{electrolyte}}$ for DME + LiFSI (1 mol kg⁻¹) and DMC + EC (1:1 wt) + LiPF₆ (1 mol kg⁻¹).

Appendix D. Measurement of t_+ with potentiostatic polarization method

The t_+ can be evaluated by applying a small voltage bias (ΔV) between the two Li metal electrodes with the swollen film in the middle (Figure D1), and by measuring the steady-state current (I_{ss}) under the assumption that only Li^+ moves at the steady state. The t_+ can be calculated from:⁵

$$t_+ = \frac{I_{ss}(\Delta V - I_0 R_{\text{int},0})}{I_0(\Delta V - I_{ss} R_{\text{int},ss})} \quad (\text{D1})$$

I_0 is the initial current at the beginning of the polarization step, which can be calculated from the Ohm's law:

$$I_0 = \frac{\Delta V}{R_{\text{bulk}} + R_{\text{int},0}} \quad (\text{D2})$$

All the resistance terms in Equation (D1) and (D2) can be evaluated from the impedance spectra before and after each polarization step. In this study, we used the equivalent circuit shown in Figure D2 to fit with the experimental results.

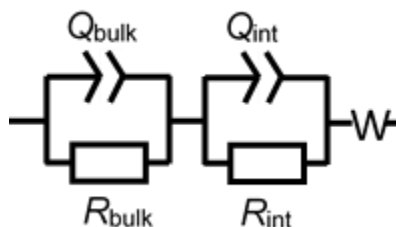


Figure D2. Equivalent circuit for the fitting of PEIS shown in Figure S8 and S9.

Q_{bulk} , and Q_{int} represent the constant phase element (CPE) of the bulk film, and the interface between the film and the Li metal, respectively. Similarly, R_{bulk} , and R_{int} represents the bulk, and interface resistance, respectively. W represents the Warburg element, accounting for the diffusion process.

The impedance spectra and the current during the polarization are shown in Figure S8 (the film swollen in DME + LiFSI) and S9 (the film swollen in DMC + EC + LiPF_6). The fitted values of R_{bulk} and R_{int} are shown in Table D. We confirmed the ionic conductivity calculated from R_{bulk} (with Li-metal non-blocking electrode) agrees with the conductivity evaluated with stainless-steel blocking electrode.



Figure D1. Scheme of the cell for the t_+ measurement

Table D. Electrode area, thickness of the swollen film, R_{bulk} , R_{int} , and t_+ , which are evaluated from Figure S8 and S9. The ionic conductivity calculated from R_{bulk} with Li-metal non-blocking electrode (σ_{Li}) agrees with the value evaluated with stainless-steel blocking electrode (σ_{S}). The error interval represents the standard deviation of the results obtained from the different voltage biases.

Electrolyte	Li ₂ S ₃ /AN (mol/mol)	Area (cm ²)	Thickness (mm)	R_{bulk} (Ω)	R_{int} (Ω)	t_+	σ_{Li} (S cm ⁻¹)	σ_{S} (S cm ⁻¹)
DME	0.1	0.71	0.097	10.4 ± 0.1	477 ± 15	0.13 ± 0.04	1.3 × 10 ⁻³	1.6 × 10 ⁻³
DME	0.2	2.0	0.26	4.9 ± 0.1	72 ± 8	0.18 ± 0.03	2.7 × 10 ⁻³	1.5 × 10 ⁻³
DME	0.3	2.0	0.11	11.3 ± 0.3	100 ± 3	0.24 ± 0.02	5.2 × 10 ⁻⁴	5.3 × 10 ⁻⁴
DME	0.4	2.0	0.13	52 ± 4	240 ± 20	0.39 ± 0.04	1.3 × 10 ⁻⁴	1.3 × 10 ⁻⁴
DME	0.6	1.3	0.12	304 ± 3	262 ± 9	0.45 ± 0.06	3.1 × 10 ⁻⁵	5.4 × 10 ⁻⁵
DME	1.0	1.3	0.097	608 ± 6	320 ± 20	0.54 ± 0.06	1.2 × 10 ⁻⁵	3.1 × 10 ⁻⁵
DMC/EC	0.1	0.71	0.10	91 ± 3	232 ± 2	0.30 ± 0.01	1.6 × 10 ⁻⁴	2.1 × 10 ⁻⁴
DMC/EC	0.2	0.71	0.11	244 ± 3	360 ± 7	0.44 ± 0.02	6.6 × 10 ⁻⁵	1.1 × 10 ⁻⁴
DMC/EC	0.3	0.71	0.11	820 ± 20	375 ± 2	0.55 ± 0.02	1.8 × 10 ⁻⁵	2.9 × 10 ⁻⁵
DMC/EC	0.4	0.71	0.048	1440 ± 40	183 ± 5	0.63 ± 0.05	4.7 × 10 ⁻⁶	4.8 × 10 ⁻⁶
DMC/EC	0.6	0.71	0.20	6.7 × 10 ⁵ ^a	1.7 ± 0.5 × 10 ⁴	0.58 ± 0.09	-	4.2 × 10 ⁻⁷

a. R_{bulk} was estimated from the conductivity test measured with stainless-steel blocking electrodes, because R_{bulk} and R_{int} were indistinguishable from the Nyquist plot.

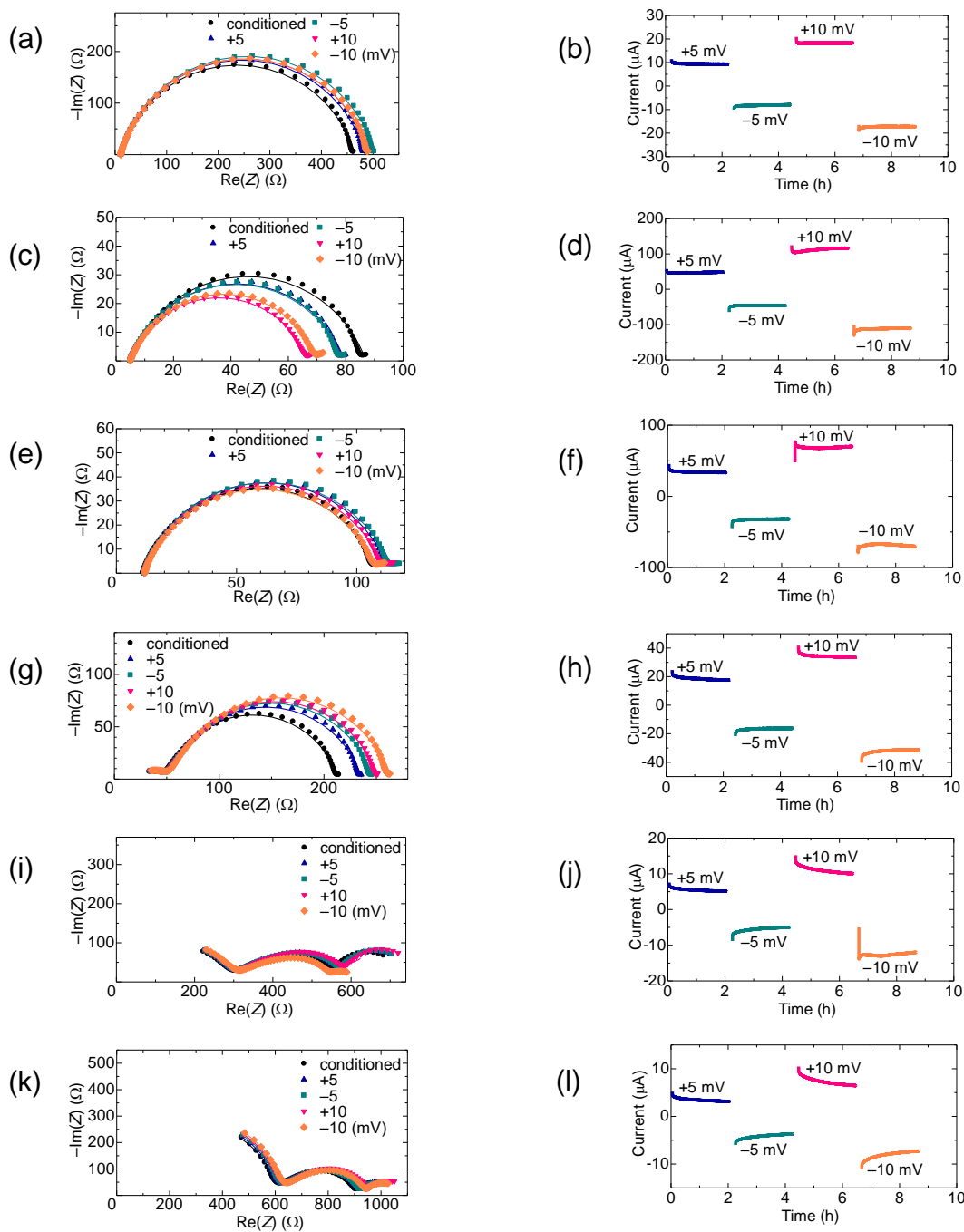


Figure S8. Potentiostatic electrochemical impedance spectra (PEIS: a, c, e, g, i, k) and chronoamperometry (CA: b, d, f, h, j, l) of PAN-PBD film swollen in DME + LiFSI (1 mol kg^{-1}). The film is cross-linked under the $\text{Li}_2\text{S}_3/\text{AN}$ ratio = 0.1 (a, b); 0.2 (c, d); 0.3 (e, f); 0.4 (g, h); 0.6 (i, j); 1.0 (k, l). The EIS is measured after the condition cycle, and at the end of each CA step. The CA is measured under the constant potential of ± 5 , ± 10 mV vs. Li^+/Li for 2 hours. The lines in the EIS represents the fitting curve to the equivalent circuit shown in Appendix D.

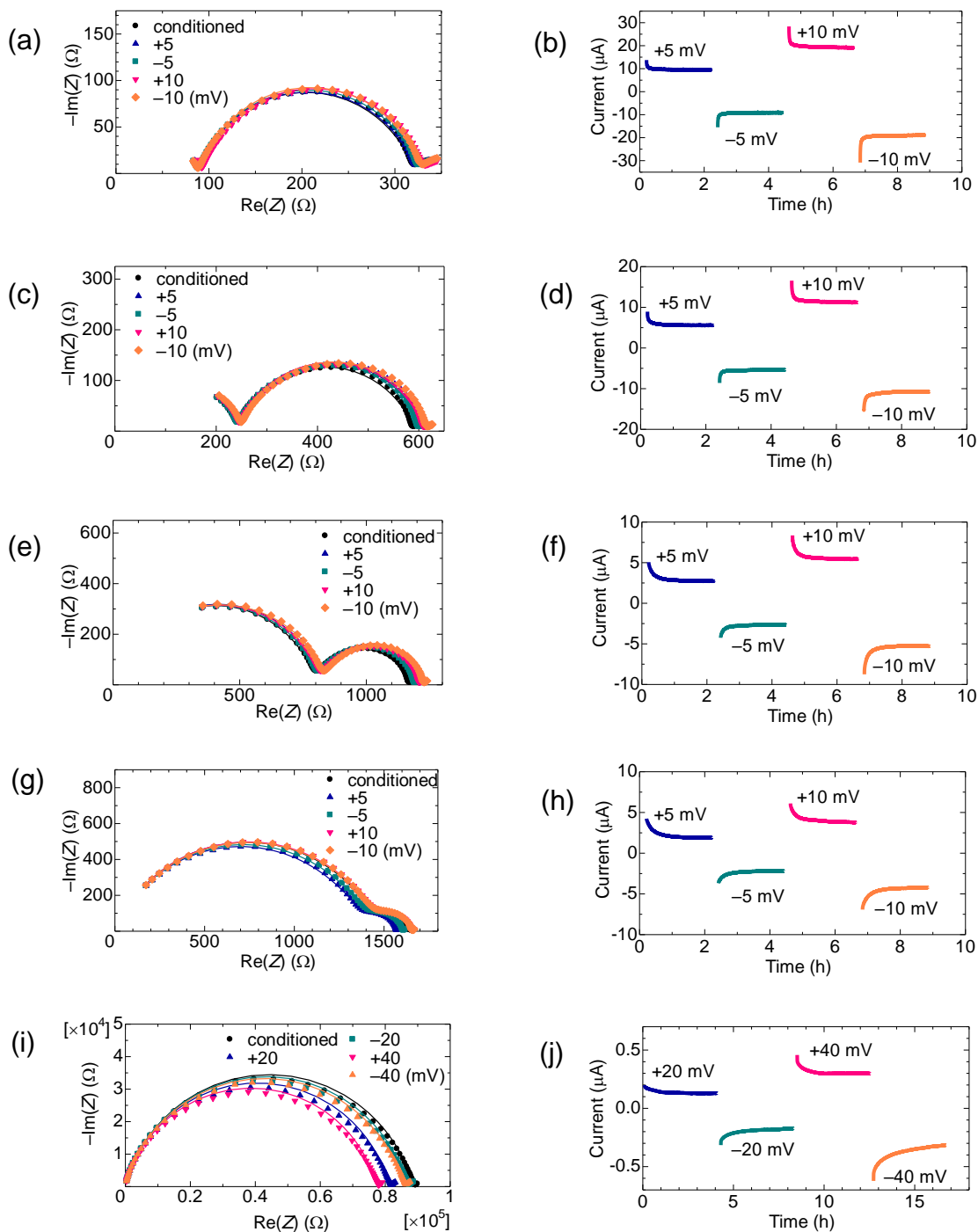


Figure S9. PEIS (a, c, e, g, i) and CA (b, d, f, h, j) of PAN-PBD film swollen in DMC + EC (1:1 wt) + LiPF_6 (1 mol kg^{-1}). The film is cross-linked under the $\text{Li}_2\text{S}_3/\text{AN}$ ratio = 0.1 (a, b); 0.2 (c, d); 0.3 (e, f); 0.4 (g, h); 0.6 (i, j). The EIS is measured after the condition cycle, and at the end of each CA step. The CA is measured under the constant potential of ± 5 , ± 10 mV vs. Li^+/Li for 2 hours (b, d, f, h), or ± 20 , ± 40 mV for 4 hours (j) because of the low conductivity of the sample. The lines in the EIS represents the fitting curve to the equivalent circuit shown in Appendix D.

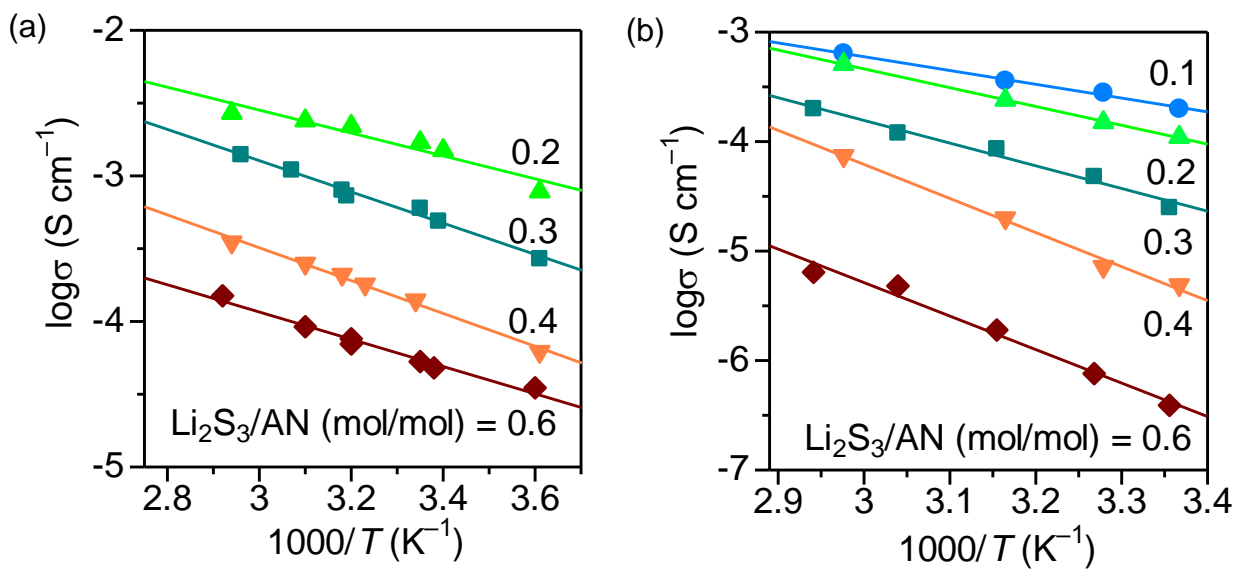


Figure S10. Arrhenius plot of PAN-PBD swollen in (a) DME + LiFSI (1 mol kg⁻¹), and in (b) DMC + EC (1:1 wt) + LiPF₆ (1 mol kg⁻¹)

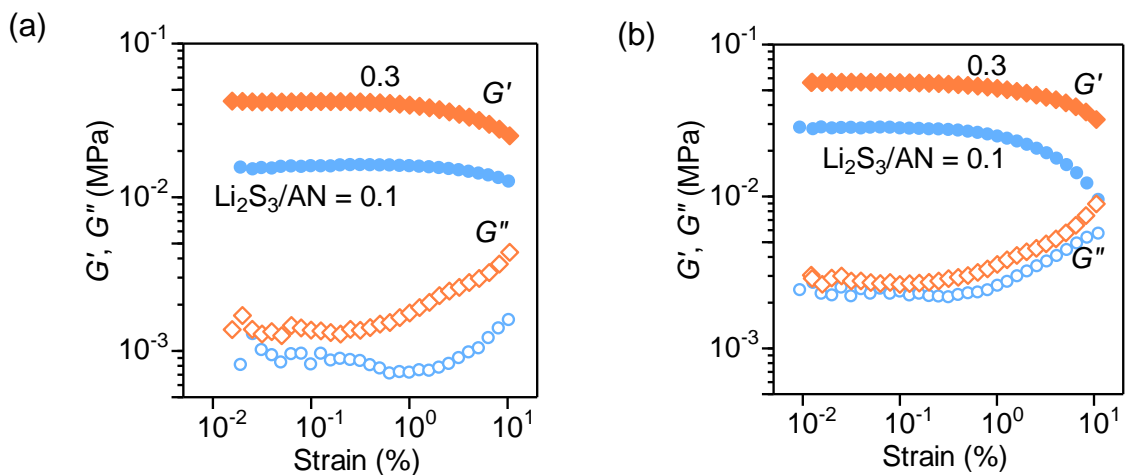


Figure S11. Strain dependence of storage (G') and loss (G'') modulus of PAN-PBD swollen in (a) DME + LiClO_4 (sat. 0.3 mol kg^{-1}), and in (b) DMC + EC (1:1) + LiClO_4 (1 mol kg^{-1}), evaluated under a constant frequency of 1Hz. The linear viscoelastic regime is evaluated as a strain range in which the G' is constant (i.e. strain $< 1\%$ in this study).

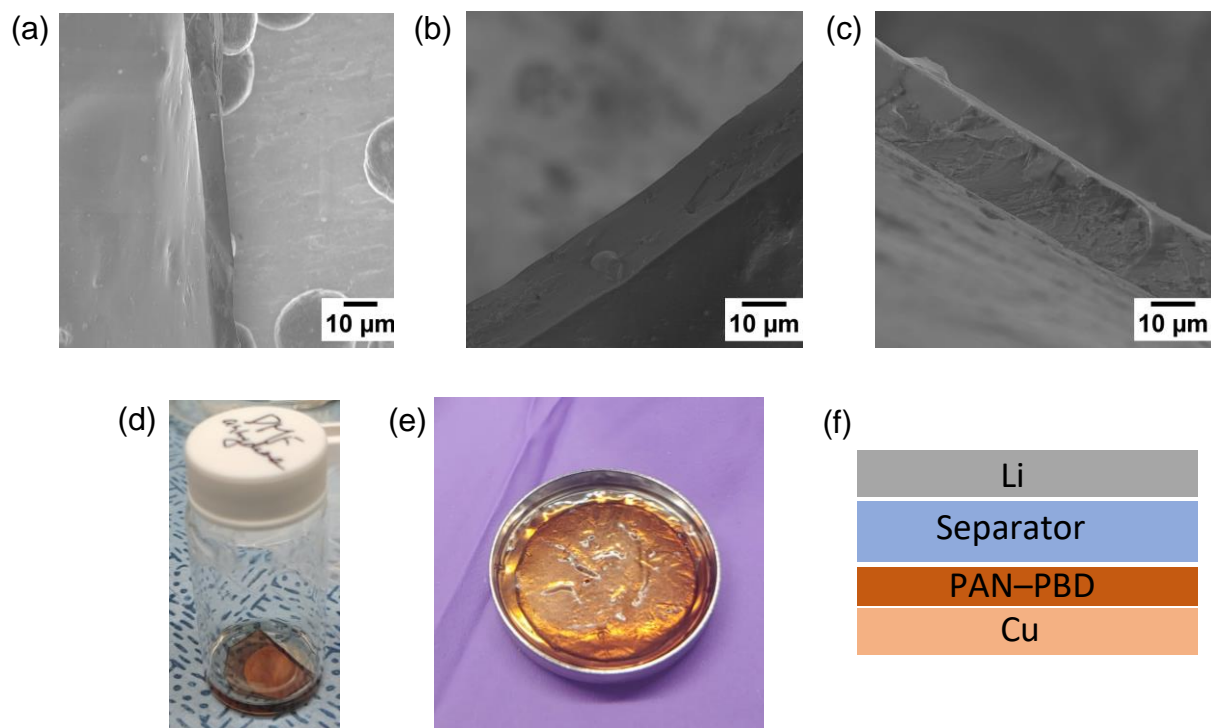


Figure S12. (a–c) Cross-sectional images of PAN–PBD thin film used as the protective coating for Li metal anode. $\text{Li}_2\text{S}_3/\text{AN} = 0.1$ (a), 0.2 (b), 0.4 (c). (d) PAN–PBD thin film peeled off from the stainless-steel substrate by immersing in DMF. (e) Free-standing PAN–PBD thin film transferred on Cu foil after thorough rinsing in DMC. (f) Cell configuration used in the Li deposition on PAN–PBD-coated Cu. The coating is fully swollen in the electrolyte (DMC + EC (1:1) + LiPF_6 (1 mol kg^{-1}) + FEC (5wt%)) prior to the cell assembly. A commercial battery separator (Celgard) is placed on top of the coating.

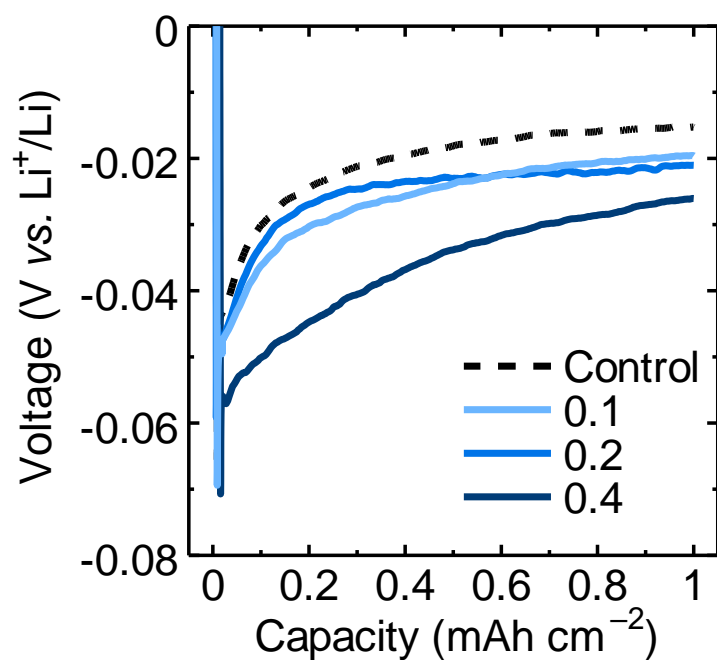


Figure S13. Voltage profiles during the first deposition of Li metal on uncoated Cu (control cell), and PAN-PBD-coated Cu ($\text{Li}_2\text{S}_3/\text{AN} = 0.1, 0.2, 0.4$). Current density = 0.1 mA cm^{-2} . The optical images of the Li metal after the deposition are shown in Figure S14.

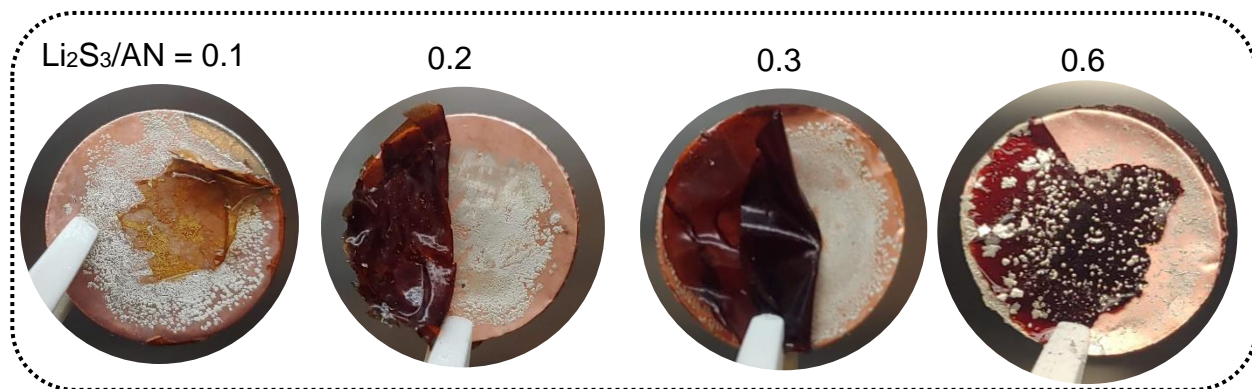


Figure S14. Optical images of Li metal underneath the PAN-PBD coating after the first deposition on Cu foil. Current density = 0.1 mA cm^{-2} , deposition capacity = 1 mAh cm^{-2} . The morphology of the Li metal is shown in Figure S15.

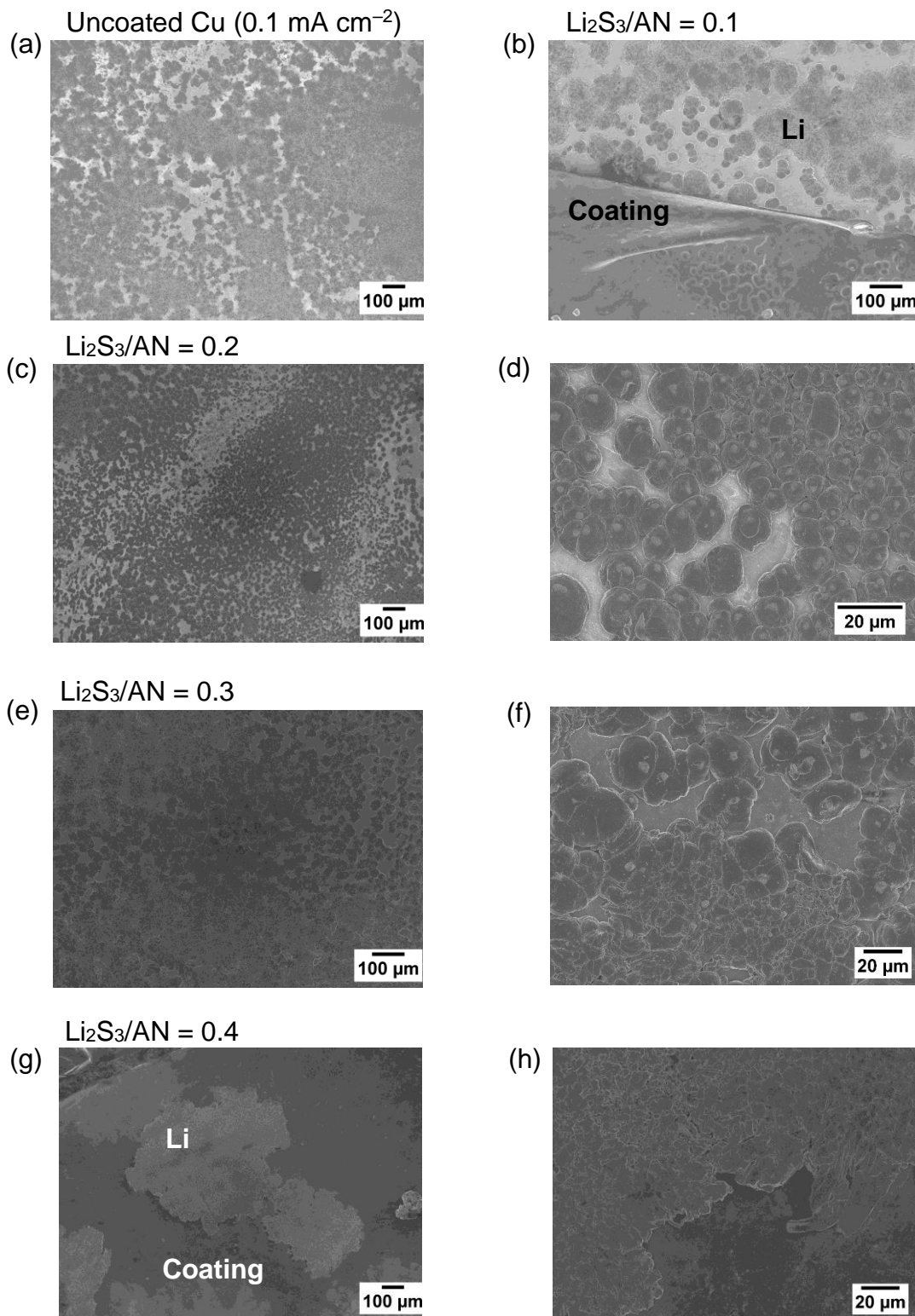


Figure S15. SEM images of Li metal after the first deposition on (a) uncoated Cu, and on (b–h) Cu with PAN–PBD coating cross-linked at $\text{Li}_2\text{S}_3/\text{AN} = 0.1$ (b); 0.2 (c, d); 0.3 (e, f); 0.4 (g, h). Li metal is deposited underneath the coating in (b–f), and on the surface in (g, h). Current density = 0.1 mA cm^{-2} , deposition capacity = 1 mAh cm^{-2} .

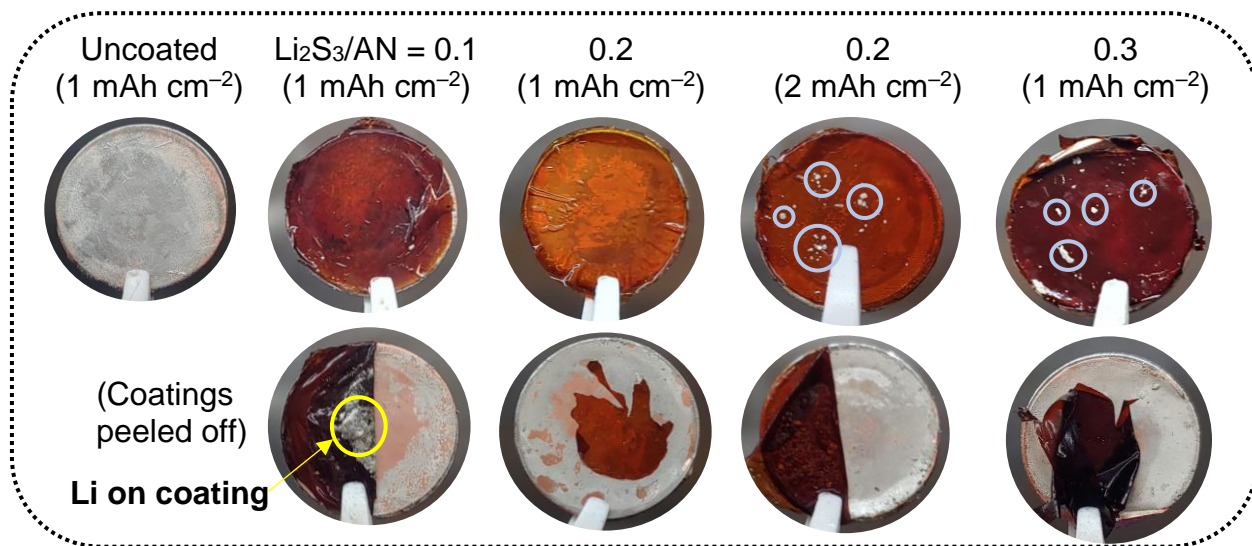


Figure S16. Optical images of Li metal after the first deposition on uncoated Cu, and on Cu with PAN-PBD coating cross-linked at $\text{Li}_2\text{S}_3/\text{AN} = 0.1\text{--}0.3$. The highlighted region shows the Li metal adhered on the backside of the coating when peeled off. Li metal plating on the coating surface is observed at $\text{Li}_2\text{S}_3/\text{AN} = 0.3$, and when the capacity is increased to 2 mAh cm^{-2} ($\text{Li}_2\text{S}_3/\text{AN} = 0.2$). Current density = 0.5 mA cm^{-2} . The morphology of the Li metal is shown in Figure S17.

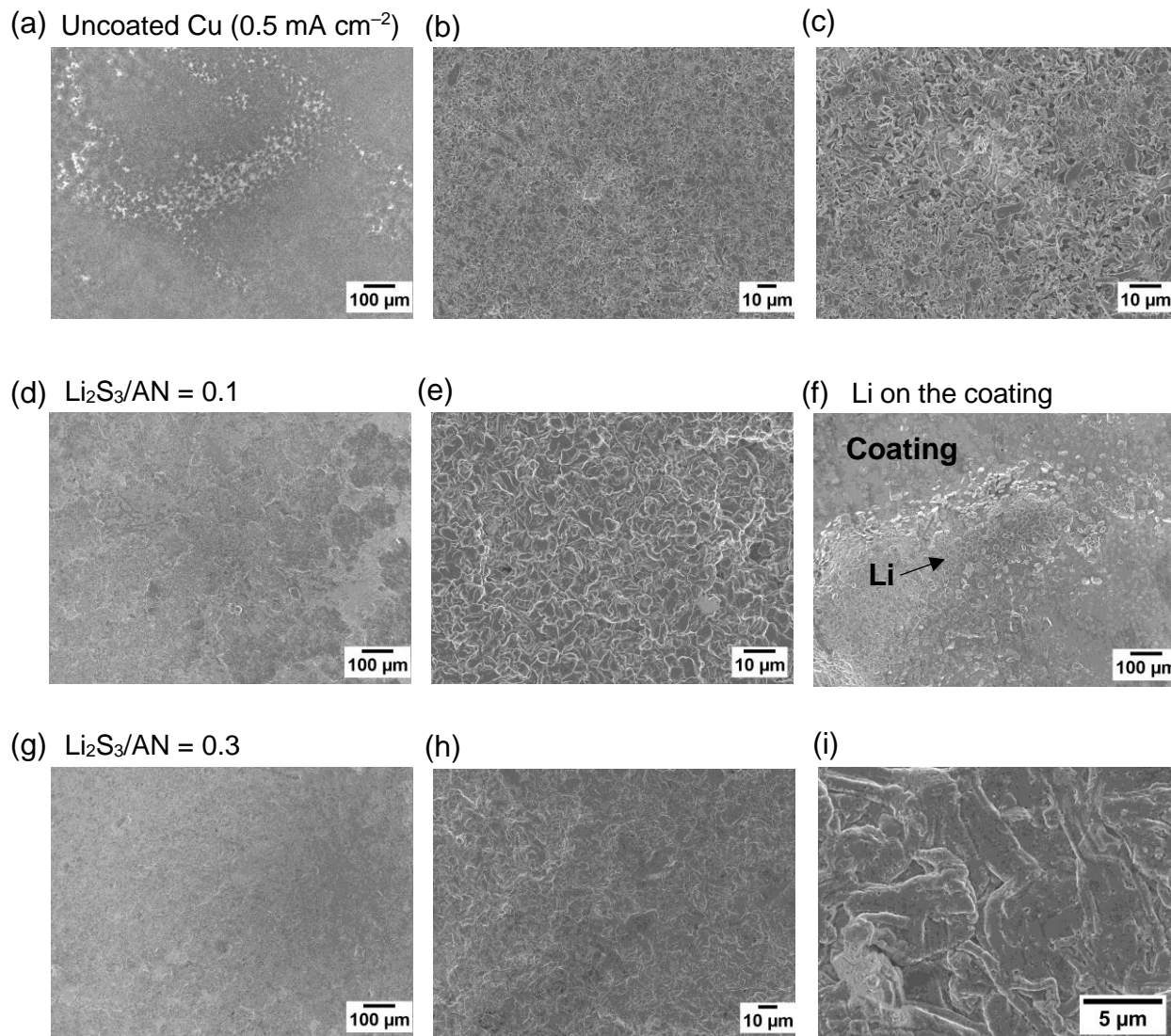


Figure S17. SEM images of Li metal after the first deposition on (a–c) uncoated Cu, and on (d, e, g–i) Cu with PAN–PBD coating cross-linked at $\text{Li}_2\text{S}_3/\text{AN} = 0.1$ (d, e); 0.3 (g–i). (f) Li metal adhered on the coating ($\text{Li}_2\text{S}_3/\text{AN} = 0.1$). Current density = 0.5 mA cm^{-2}

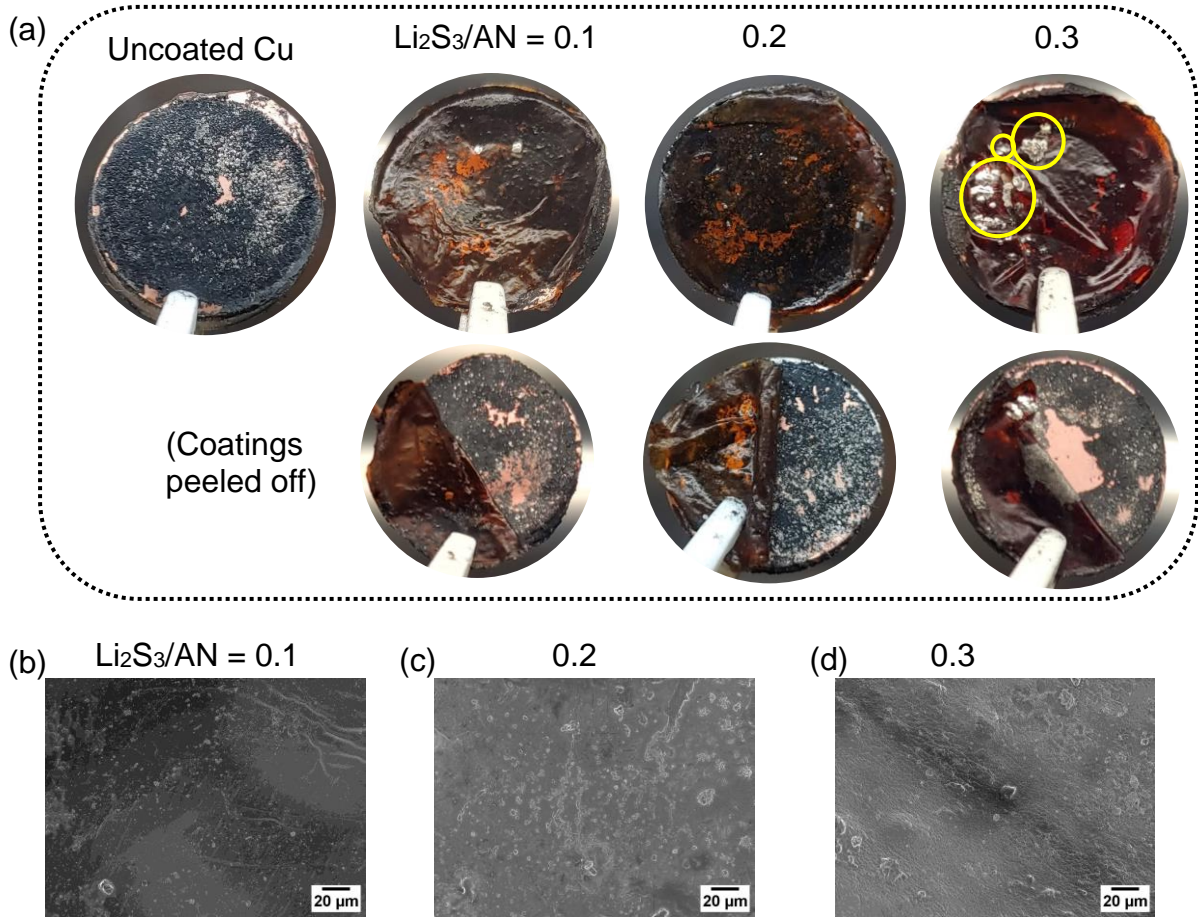


Figure S18. (a) Optical images of Li metal after the 51st deposition on uncoated Cu, and on Cu with PAN-PBD coating ($\text{Li}_2\text{S}_3/\text{AN} = 0.1\text{--}0.3$). The highlighted area shows Li metal plating on the coating surface at $\text{Li}_2\text{S}_3/\text{AN} = 0.3$. (b–d) SEM images of the PAN-PBD coating after 50 cycles of Li deposition/dissolution. Current density = 0.1 mA cm^{-2} , deposition capacity = 1 mAh cm^{-2} .

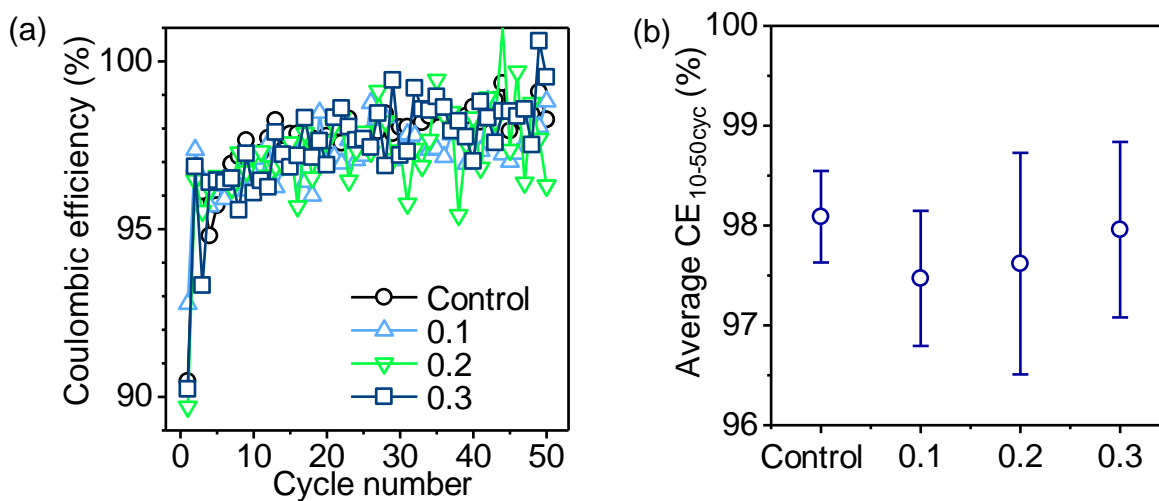


Figure S19. (a, b) Coulombic efficiency (CE) of Li metal deposition/dissolution on uncoated Cu (control), and on PAN-PBD-coated Cu ($\text{Li}_2\text{S}_3/\text{AN} = 0.1\text{--}0.3$). (a) CE at each cycle, (b) average CE between 10 and 50 cycle. The error bar represents the standard deviation. Current density = 0.1 mA cm^{-2} , deposition capacity = 1 mAh cm^{-2} .

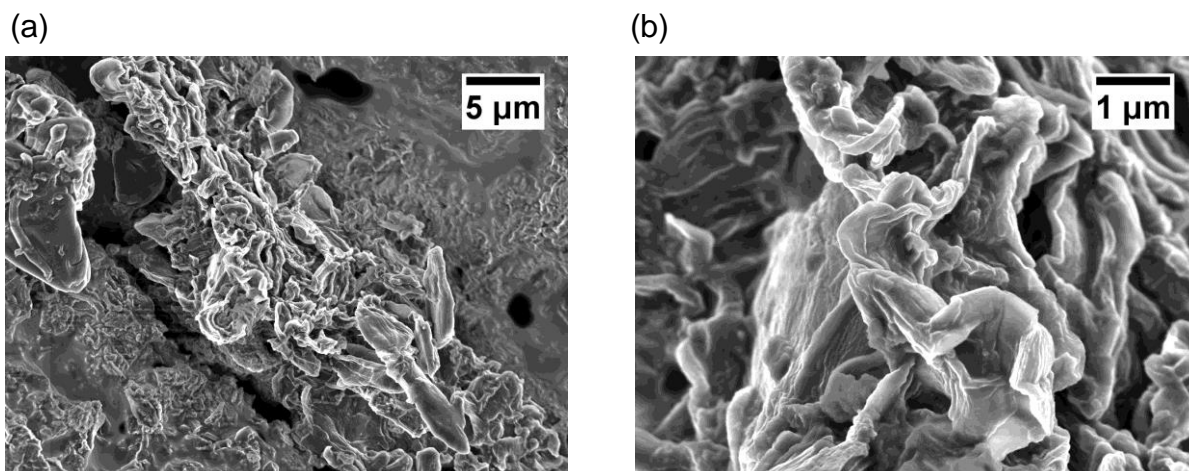


Figure S20. (a, b) SEM images of Li metal after the 51st deposition on PAN-PBD-coated Cu ($\text{Li}_2\text{S}_3/\text{AN} = 0.3$). The sample in the image is the Li deposits adhered on the Cu-side of the coating surface as shown in Figure S18. Current density = 0.1 mA cm^{-2} , deposition capacity = 1 mAh cm^{-2} .

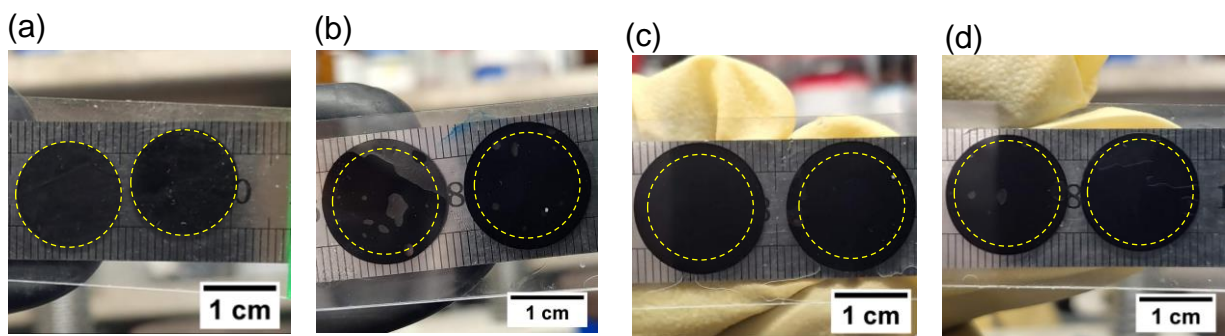


Figure S21. Optical images used for the evaluation of the swelling ratio: (a) dry film (b) swollen in pure DMC (c) in DMC/EC (1:1) (d) in DMC/EC/LiPF₆ (1 mol kg⁻¹) The circle in the images represents the area of the dry film (a). Sample in image: Li₂S₃/AN = 0.3

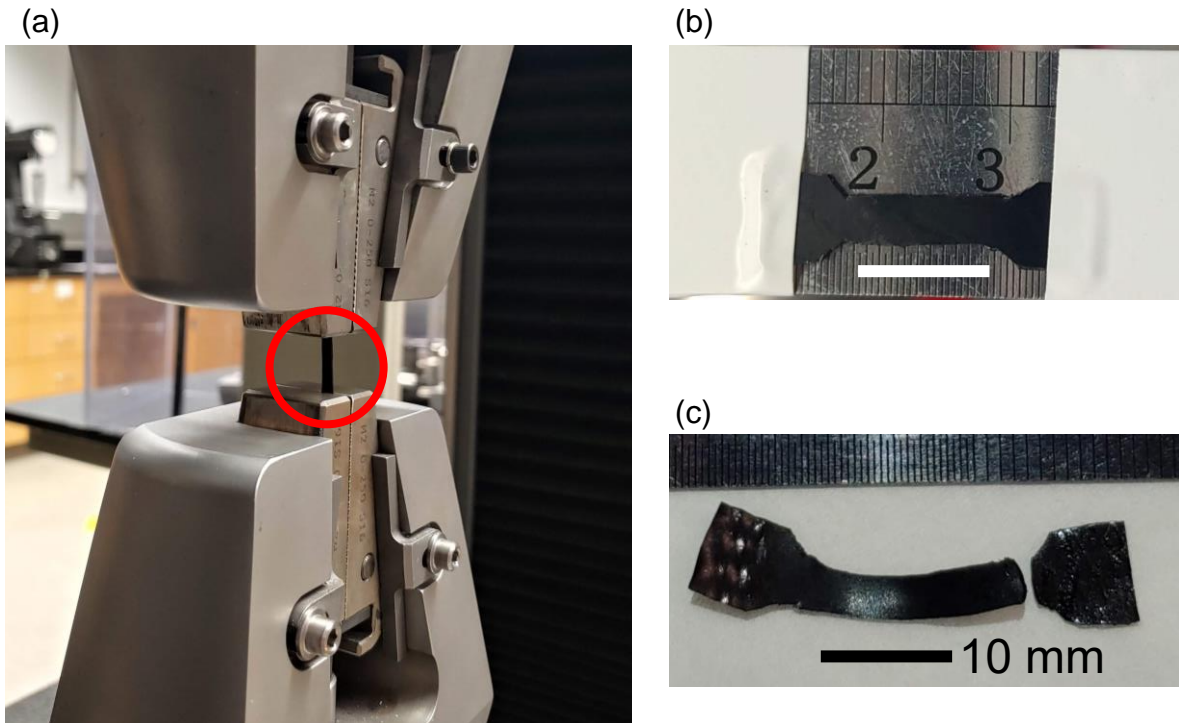


Figure S22. Photograph of the tensile test of the dry PAN–PBD film: (a) the film clipped to the instrument (b) the film before the tensile test and (c) after the break. The dimension of the sample is 10 mm (length) \times 4 mm (width) \times 0.5 ± 0.2 mm (thickness). Sample in image: $\text{Li}_2\text{S}_3/\text{AN} = 0.6$

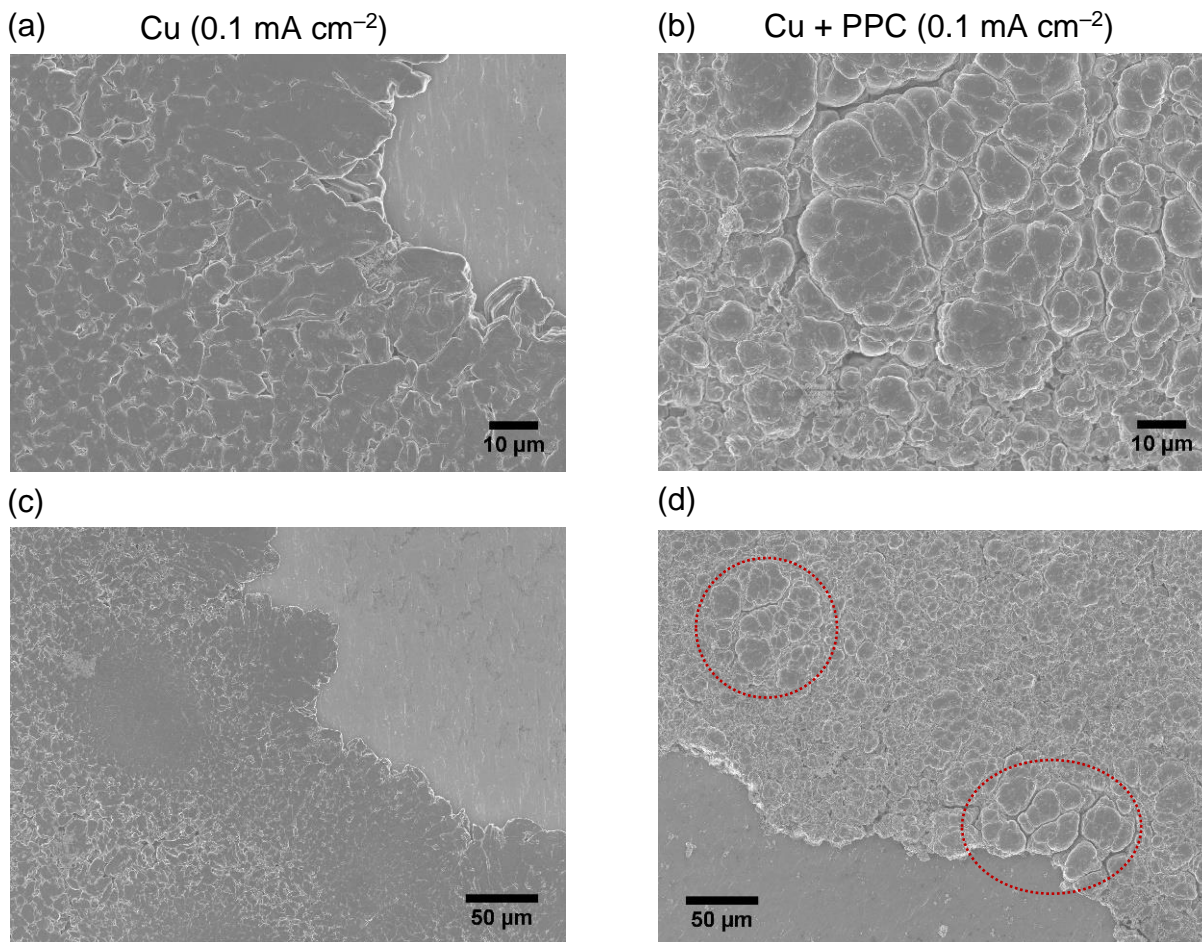


Figure S23. SEM images of Li metal deposited on Cu foil in the ether LE ($\text{DME} + 1 \text{ mol kg}^{-1} \text{ LiFSI}$). (a, c) without the PPC (b, d) with the PPC ($\text{Li}_2\text{S}_3/\text{AN} = 0.1$). The spherical morphologies of Li metal can be observed under the PPC layer (circled areas). Current density = 0.1 mA cm^{-2} , capacity = 1 mAh cm^{-2} .

References

- (1) Sato, S.; Honda, Y.; Kuwahara, M.; Kishimoto, H.; Yagi, N.; Muraoka, K.; Watanabe, T. Microbial Scission of Sulfide Linkages in Vulcanized Natural Rubber by a White Rot Basidiomycete, *Ceriporiopsis s Ubvermispora*. *Biomacromolecules* **2004**, *5* (2), 511–515. <https://doi.org/10.1021/bm034368a>.
- (2) Hansen, C. M. *Hansen Solubility Parameters*, 2nd Editio.; CRC Press, 2007. <https://doi.org/10.1201/9781420006834>.
- (3) Lindvig, T.; Michelsen, M. L.; Kontogeorgis, G. M. A Flory-Huggins Model Based on the Hansen Solubility Parameters. *Fluid Phase Equilib.* **2002**, *203* (1–2), 247–260. [https://doi.org/10.1016/S0378-3812\(02\)00184-X](https://doi.org/10.1016/S0378-3812(02)00184-X).
- (4) Croll, S. G. Application of the Flory-Rehner Equation and the Griffith Fracture Criterion to Paint Stripping. *J. Coatings Technol. Res.* **2010**, *7* (1), 49–55. <https://doi.org/10.1007/s11998-009-9166-4>.
- (5) Pesko, D. M.; Sawhney, S.; Newman, J.; Balsara, N. P. Comparing Two Electrochemical Approaches for Measuring Transference Numbers in Concentrated Electrolytes. *J. Electrochem. Soc.* **2018**, *165* (13), A3014–A3021. <https://doi.org/10.1149/2.0231813jes>.